FAULT LOCATION WITH DGs IN RADIAL DISTRIBUTION SYSTEM USING RADIAL BASIS FUNCTION NEURAL NETWORK

Saifulnizam Abd Khalid[1*], Muhammad Hafiiz Hamzah[1], and Ahmad Ridhwan Wahap[1]

[1]School of Electrical Engineering, Faculty of Engineering, Universiti Teknologi Malaysia, 81310 UTM Johor Bahru, Johor, Malaysia

Corresponding author* email: saifulnizam@utm.my
Accepted 1 November 2021, available online December 2021

ABSTRACT

Increasing penetration of Renewable Energy in energy market will contribute to increasing number of distributed generation (DG) existence in the grid, thus leading to conflict in fault location, detection and protection coordination in distribution system. This study is focuses on single-line-to-ground (LG) fault detection in a radial distribution system. The objective of this study is to estimate fault location in a radial distribution system in the presence of DGs by using Radial Basis Function Neural Network (RBFNN), with consideration to minimize monitor placement in system. Fault location has been estimated in term of faulty bus. Two types of radial distribution network with DGs have been tested in this study; 10 bus and 34 bus network. Fault analysis has been performed using Power World simulator and data generated has been applied for RBFNN development via MATLAB. RBFNN performance was then evaluated statistically, by SSE, R^2 and RMSE. The proposed RBFNN has been able to accurately predict current magnitude at unmonitored buses by only few provided monitored buses readings. With accurate predicted results by the neural network, pattern of current magnitude during fault has been observed in order to identify faulty buses. It was shown in this study that faulty bus can be identified 100% using the proposed approach.

Keywords: Radial distribution system, distributed generation, single-line-to-ground fault, radial basis function neural network, minimum monitor placement

1. Introduction

Electrical power transmission and distribution network need to be expanded as the demand and dependencies on electricity is increasing [1] [2] [3]. This results to more complex transmission and distribution network. Power providers need to cater customer demands for a continuous supply without interruptions. Fault occurrences may lead to power system failure. An effort on how to overcome and prepare for fault in maintaining system security becomes an extremely important task.

It is necessary to foresee the interruptions that may occur in the distribution system by detecting failures and to isolate only the faulty sections. Fault location identification need to be accurate to ensure safe and good selectivity of a protection scheme. Identification need to be fast for any protection actions or measures to be taken in a faulty power system. There are many method found to be effective in fault location identification. Impedance-based method and travelling wave method are some example of methods which have been developed in previous studies [5] [6] [7]. However, with advancement in microprocessor and computer technology nowadays, fault location detection method has been evolving from conventional analysis method to a better method, using artificial intelligence (AI). AI application has been recently increased due to its accuracy and fast response time.

Based on statistics of previous study on asymmetrical faults, more than 70% of faults occurring in distribution system are single-line-to-ground (LG) faults [6]. Based on this statistical figure, priority to solve LG fault location and identification issue is higher than other type of faults.

Meanwhile, installation of on-grid renewable energy system led to introduction of Distributed Generation (DG) into national electricity grid. DG is an installation of a generating unit at a strategic point of location [8], purposely to let electricity distribution to be more dynamic and efficient. With DGs, electricity delivery losses can be reduced (increased reliability) [9], and in some countries, consumer can enjoy benefit by selling excess power to grid [10].

There are four main categories in fault location detection method; technique based on impedance measurement [5] [6], technique based on travelling-wave phenomenon [4] [7] [14] [15] [16], technique based on currents and voltages high frequency components and knowledge-based technique [11] [12] [17] [18].

Artificial Neural Network (ANN) and fuzzy logic are among the best example of knowledge-based technique in automated fault location detection.

Author [12] and [18] suggested that voltage sag can be an indicator for fault location detection. Author [18] suggested a method applying ANN with Levenberg-Marquardt Back propagation method to detect fault location in a transmission network. Voltage deviation index has been calculated and been used to train ANN via MATLAB. In [12], author also suggested to consider voltage sag by voltage deviation index as a figure to determine fault location. Radial Basis Function Neural Network (RBFNN) has been proposed because it can generate fast and accurate results. Voltage deviation index has been used to train RBFNN via MATLAB. Even by applying different algorithm concept of ANN application, both [12] and [18] shows a very high accuracy in result.

However, in a radial distribution network, consideration of only voltage value to determine fault location was found to be not suitable. In a ring distribution system, pre-fault voltage at all feeders may be considered at the same magnitudes. Therefore, any voltages disruption or fluctuation due to fault in a ring system can be identified clearly. On the other hand, in a radial distribution network where the pre-fault voltage value of all bus was not same; dropped as bus distance from source is increased, voltage fluctuation or disruption due to fault may be difficult to distinguish.

RBFNN approach for fault location scheme by fault current level measurement in a distribution network with DGs has been suggested in [11]. Three stage of RBFNN has been developed. The first stage is to determined type of fault by normalized current calculation. The second stage is to determine fault location and the third stage to activate which circuit breaker to isolate the faulty line. Fault location detection algorithm is by applying back propagation method. However, huge quantity of monitor may be required for data capturing to implement the suggested scheme into actual network which may consists of hundreds or thousands of buses. Monitor placement method has been proposed on [13]. By considering monitor placement, monitor quantity to estimate fault location in system was expected can be minimized.

ANN was chosen as a method for fault location detection for this study considering low accuracy of other fault location detection technique compared to knowledge-based technique, and to achieve fast computation time to locate fault. Furthermore, due to Radial Basis Neural Network (RBFNN) performance which can produce more fast and accurate result compared to other ANN method, RBFNN is proposed to be applied in this study. In addition, to obtain a cost friendly fault location detection scheme for the industry, monitor placement has been considered to minimize monitor placement quantity.

2. Methodology

Four types of test models have been applied in developing and verifying RBFNN for current magnitude prediction at buses during LG fault. Fault analysis has been carried out using Power World simulator, and RBFNN has been developed using nntool of MATLAB. RBFNN prediction results have been evaluated statistically using SSE, R^2 and RMSE. Prediction data were then arranged into table. Data pattern has been analyzed in order to identify the faulty bus in a radial distribution system.

2.1 Test Model

Figure 1 shows type of test model which has been applied in developing the proposed method. Total four types of test models have been applied.

Figure 1. Type of test model in this study

2.1.1 10 Bus Single Radial Distribution System Without DG

The 10 bus single radial distribution test network was based on the work of R. S. Rao et al [19]. Loads and lines data also can be found in [19].

2.1.2 10 Bus Single Radial Distribution System With DG

One unit DG has been added into bus 10 of previous 10 bus single distribution system to simulate a system with DG presence. Figure 2 shows a single line of 10 bus single radial distribution test network with presence of one unit DG. DG parameter for this model as per shown in Table 1. Load and line data for this test system are similar with 10 bus single radial distribution without DG network as per shown in [19].

Figure 2. 10 bus single radial distribution system with DG

Table 1. DG parameter for 10 bus single radial distribution system with DG

DG real power [MW]	0.5
DG reactive power [Mvar]	0.37
Connecting bus	Bus 10

2.1.3 34 Bus Radial Distribution System Without DG

The third test model is 34 bus radial distribution system without DG [20]. This 11kV system has one source and four branches. The lines and loads data are based on reference [20].

2.1.4 34 Bus Radial Distribution System With DGs

The single line diagram of 34 bus radial distribution system with DG is depicted in Figure 3. DGs parameters for this system are shown in Table 2. Meanwhile, load and line data for this test system are similar with 34 bus radial distribution system without DG as per reference [20].

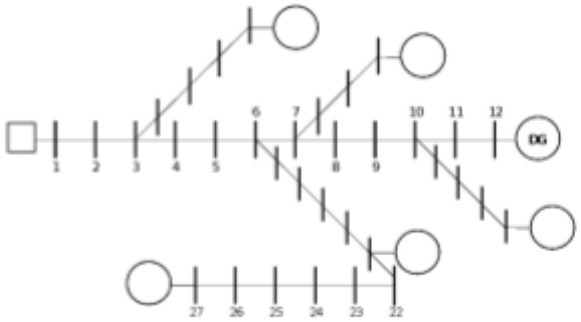

Figure 3. 34 bus radial distribution system with DG

Table 2 DG parameter for 34 bus radial distribution system with DGs

DG number	Connect bus number	P_{DG} [MW]	Q_{DG} [Mvar]
1	12	0.50	0.37
2	16	0.50	0.37
3	21	0.50	0.37
4	27	0.50	0.37
5	30	0.50	0.37
6	34	0.50	0.37

2.2 Power World Simulation

Fault analysis has been conducted using Power World simulator for the above four test models in order to obtain current magnitude value at all buses during LG fault. Fault analysis was carried out with pre fault profile of Flat IEC-909, and voltage setting 1.0000 p.u.

Fault analysis was repeated with fault resistance (R_f) value of 0 Ω (bolted fault), 0.05 Ω, 0.1 Ω, 0.15 Ω, 0.2 Ω and 0.25 Ω. While for 34 bus radial distribution with DGs only, fault analysis was repeated with fault resistance (R_f) value of 0 Ω (bolted fault), 0.05 Ω, 0.1 Ω, 0.15 Ω, 0.2 Ω, 0.25 Ω and 0.3 Ω.

2.3 RBFNN Development

RBFNN has been developed using neural network toolbox (nntool) via MATLAB R2013a software. Exact radial basis (newrbe) function analysis has been applied for development. Three parameters was set in developing RBFNN, namely input vector, output vector and spread constant.

Figure 4 shows overall process flow in developing the faulty bus detection scheme for this study. Current magnitude at buses data (obtained from Power World simulator fault analysis) has been arranged into table accordingly in order to identify pattern of data. Considering system topology and current magnitude pattern, monitored and unmonitored buses has been selected. Monitored buses data will be applied as input vector, while unmonitored buses data will be applied as output (or target) vector for RBFNN training. In application, the proposed RBFNN will need to predict unmonitored buses current magnitude by only few monitored buses current magnitude. To have a greater accuracy of predicted data, the most suitable spread constant for the proposed RBFNN has been selected.

Current magnitude data with various R_f has been applied for RBFNN training as per below Table 3. Meanwhile, monitored bus data of R_f 0.15 Ω has been used as test sample to verify the trained RBFNN whether it can accurately predict unmonitored buses current magnitude values or not.

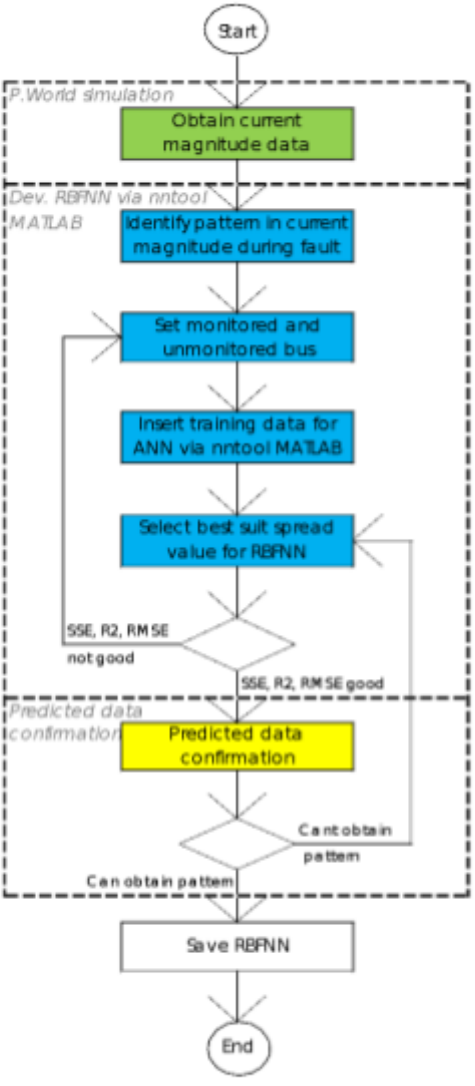

Figure 4. Process flow to develop the proposed scheme

Table 3. Data for RBFNN training and testing

Test model	RBFNN training data	RBFNN testing data
10 bus without DG 10 bus with DG 34 bus without DG	Current magnitude data of; $R_f = 0\ \Omega$ $R_f = 0.05\ \Omega$ $R_f = 0.1\ \Omega$ $R_f = 0.2\ \Omega$ $R_f = 0.25\ \Omega$	Current magnitude data of; $R_f = 0.15\ \Omega$
34 bus with DG	Current magnitude data of; $R_f = 0\ \Omega$ $R_f = 0.05\ \Omega$ $R_f = 0.1\ \Omega$ $R_f = 0.2\ \Omega$ $R_f = 0.25\ \Omega$ $R_f = 0.3\ \Omega$	Current magnitude data of; $R_f = 0.15\ \Omega$

2.4 Results Evaluation

In order to obtain a RBFNN which can accurately predict unmonitored buses current magnitudes, the spread constant need to be chosen correctly. The spread constant values have been selected based on the best sum of square error (SSE), coefficient of determination (R^2) and root mean square error (RMSE) results among all tested spread constant values. SSE, R^2 and RMSE have been calculated by the following formulae [21];

$$SSE = \sum_{i=n}^{n} (\hat{y}_i - y_i)^2 \tag{2.1}$$

$$R^2 = 1 - \frac{\sum_{i}^{n} (\hat{y}_i - y_i)^2}{\sum_{i=n}^{n} (\hat{y}_i - \dot{y}_i)^2} \tag{2.2}$$

$$RMSE = \sqrt{\frac{\sum_{i=n}^{n} (\hat{y}_i - y_i)^2}{n}} \tag{2.3}$$

Where,

$\hat{y}_i$ is predicted current magnitude value
$\dot{y}_i$ is the simulated current magnitude value in average
y_i is the simulated current magnitude e
is the number of dataset

Statistically, SSE and RMSE should be close to zero "0" and R^2 should be close to one "1" to prove that predicted data were accurate (RBFNN predicted values are close to the Power World simulated values).

To identify faulty bus, predicted current magnitude values of unmonitored buses during LG fault has been arranged into table. Predicted data should show a pattern to help identify faulty bus.

3. Results and Discussion

The proposed fault detection scheme was tested on 10 bus and 34 bus radial distribution system with and without DGs. Data sets of current magnitude at buses during LG fault was generated using fault analysis via Power World simulator. Generated data then has been used to develop RBFNN, and some consideration has been made to minimize monitor placement in the test system. Fault location detection has been performed in term of faulty bus identification.

3.1 10 Bus Single Radial Distribution System Without DG

Six data sets with various R_f has been generated using Power World fault analysis. Five data sets have been used for RBFNN training, while 1 data set has been used for RBFNN testing.

It was observed that, in a 10 bus system without DG, the highest observed current magnitude was during LG fault (R_f = 0 Ω) at bus 1, which was 1.000 p.u. Meanwhile, the lowest current magnitude was observed during LG fault (R_f = 0.25 Ω) at bus 10, which was 0.03174 p.u.

Referring to Appendix A Table A1, when LG fault (R_f = 0 Ω) was simulated at bus 1, monitor at bus 1 was showing 1.000 p.u, and monitor at bus 2 to 10 were showing 0 p.u. current magnitudes (see column 1). From all data sets, it can be observed that buses which comes after faulty bus show zero "0" p.u current magnitudes. All data sets are showing similar current magnitude pattern at buses during LG fault.

Figure 5 shows an explanatory image of current flows during fault in a single source radial distribution system without DG, while Figure 6 shows current magnitude at all buses during LG fault (R_f = 0) was simulated at bus 6. It was proved by fault analysis in Power World simulator that, in a single source radial distribution system without DG, fault current contribution can be seen only from source. As the faulted bus is shorted to the ground, current magnitude at buses which appear after the faulty bus will show zero p.u. current magnitude.

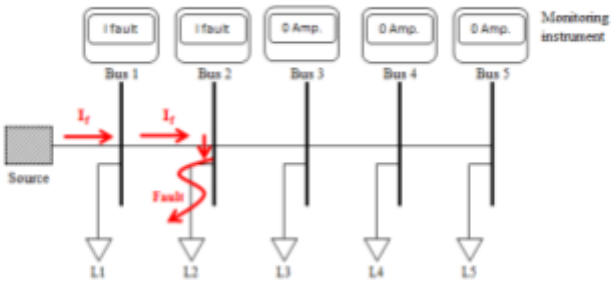

Figure 5. Explanatory image of fault current flows in a single radial system without DG

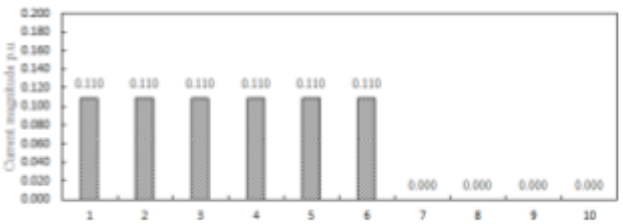

Figure 6. Current magnitude at each bus during LG fault (R_f=0) simulated at bus 6

As mentioned in previous section, RBFNN will need to predict unmonitored buses current magnitude by only few given magnitude of monitored bus. Bus 1 has then been selected as the only monitored bus needed based on current magnitude pattern shown in all data set with different R_f.

If only consider monitoring values at bus 1, current magnitude can be seen becomes smaller as the faulty bus location becomes further from the source (see row 1 of Table A1 Appendix A). When LG fault was simulated at bus 1, monitor at bus 1 shows 1.000 p.u., and when LG fault was simulated at bus 10, monitor at bus 1 shows 0.032 p.u. RBFNN will be trained to predict bus 2 to 10 current magnitudes by monitor placement at bus 1 alone. In this case, bus 1 will be set as monitored bus, while bus 2, 3, 4, 5, 6, 7, 8, 9, and 10 will be set as unmonitored buses.

RBFNN was then developed using nntool in MATLAB. Figure 7 shows the structure of RBFNN for 10 bus system without DG with 1 unit monitor placement. The numbers of neuron for input and output layers are 1 and 9, respectively. The hidden layer of radial basis contains 50 neurons while linear layer contains 9 neurons.

Figure 7. RBFNN structure for 10 bus system without DG

Table 4 shows the performance analysis of the developed RBFNN for various values of spread constant. The best spread constant for 10 bus system without DG was found to be 0.1. The best performance shows result of 2.86E-04 for SSE, 0.9998 for R^2 and 1.80E-03 for RMSE. Figure 8 shows regression plots of spread constant of 1 and 0.1 for the developed RBFNN with simulated data in x-axis and predicted data in y-axis. Referring Figure 8 (b), predicted data can be seen fit the simulated data with spread constant 0.1.

Table 4. RBFNN performance for 10 bus system without DG with different spread constant

Spread constant	SSE	R^2	RMSE
100	2.36E-01	0.7352	5.17E-02
50	4.11E-02	0.9644	2.16E-02
1	1.06E-02	0.9912	1.10E-02
0.5	2.64E-03	0.9978	5.48E-03
0.1	**2.86E-04**	**0.9998**	**1.80E-03**

Based on above results with spread constant of 0.1, RBFNN has predicted current magnitude for bus 2 to bus 10 for 10 bus system without DG accurately. Comparison of Table 5 and 6 shows that predicted current magnitude values in diagonal were very close to the simulation values. In addition, considering pattern of predicted current magnitude at buses, it can be seen that it is possible to identify faulty buses with the proposed RBFNN predicted data.

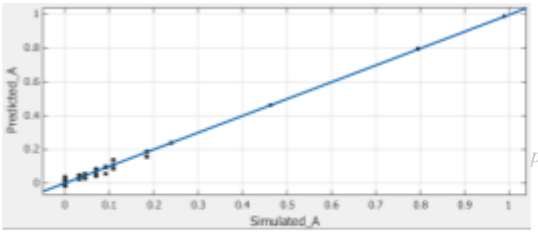

(a) Spread = 1

phy Syste

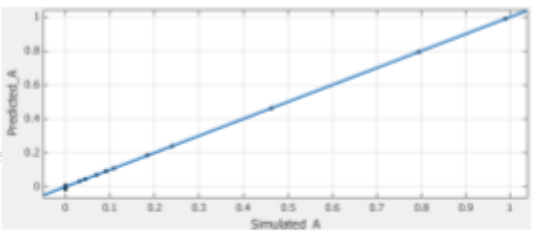

(b) Spread = 0.1

3.2 10 bus single radial distribution system with DG

Similar to previous model's approach, six data sets with various R_f has been generated using Power World fault analysis. Five data sets have been used for RBFNN training, while 1 data set has been used for RBFNN testing.

It was observed that, in a 10 bus system with DG, the highest observed current magnitude was during LG fault (R_f = 0 Ω) at bus 1, which was 1.024 p.u. Meanwhile, the lowest current magnitude was observed during LG fault (R_f = 0.25 Ω) at bus 6, which was 0.147 p.u.

Referring to Appendix B Table B1 (R_f = 0 Ω), when LG fault was simulated at bus 2 (see column 2), monitor at bus 1 was showing 0.8048 p.u, monitor at bus 2 shows 0.829 p.u., and monitor at bus 3 to 10 were showing 0.03697 p.u. current magnitudes. Based on these patterns, faulty buses can be identified by looking at the highest current magnitude in the column.

In a radial system with DG, fault current also being contributed by DG which exists in the system. Figure 9 explains about fault current flows in a system with one source and one DG. It can be seen that, fault current magnitude flowing through the faulty bus is the sum of current from source and DG during fault occurrence. This phenomenon has been proved by data generated by fault analysis which was performed earlier, as per shown in Figure 10.

Table 5. Simulated data of 10 bus system without DG for RBFNN test sample (R_f = 0.15Ω)

		Faulty bus									
		Bus 1	Bus 2	Bus 3	Bus 4	Bus 5	Bus 6	Bus 7	Bus 8	Bus 9	Bus 10
Monitoring at bus	Bus 1	**0.989**	0.79435	0.46265	0.23905	0.18411	0.1087	0.09123	0.06994	0.04478	0.03182
	Bus 2	0	**0.79435**	0.46265	0.23905	0.18411	0.1087	0.09123	0.06994	0.04478	0.03182
	Bus 3	0	0	**0.46265**	0.23905	0.18411	0.1087	0.09123	0.06994	0.04478	0.03182
	Bus 4	0	0	0	**0.23905**	0.18411	0.1087	0.09123	0.06994	0.04478	0.03182
	Bus 5	0	0	0	0	**0.18411**	0.1087	0.09123	0.06994	0.04478	0.03182
	Bus 6	0	0	0	0	0	**0.1087**	0.09123	0.06994	0.04478	0.03182
	Bus 7	0	0	0	0	0	0	**0.09123**	0.06994	0.04478	0.03182
	Bus 8	0	0	0	0	0	0	0	**0.06994**	0.04478	0.03182
	Bus 9	0	0	0	0	0	0	0	0	**0.04478**	0.03182
	Bus10	0	0	0	0	0	0	0	0	0	**0.03182**

Table 6. RBFNN predicted data of 10 bus system without DG for RBFNN test sample ($R_f = 0.15\Omega$)

		Faulty bus									
		Bus 1	Bus 2	Bus 3	Bus 4	Bus 5	Bus 6	Bus 7	Bus 8	Bus 9	Bus 10
Monitoring at bus	Bus 1	**0.989**	0.79435	0.46265	0.23905	0.18411	0.1087	0.09123	0.06994	0.04478	0.03182
	Bus 2	0	**0.7944**	0.4627	0.2391	0.1841	0.1087	0.0912	0.0699	0.0448	0.0318
	Bus 3	0	0	**0.4626**	0.239	0.1841	0.1087	0.0912	0.0699	0.0448	0.0318
	Bus 4	0	0	0	**0.239**	0.1841	0.1087	0.0912	0.0699	0.0448	0.0318
	Bus 5	-0.0011	0.0002	0	-0.0001	**0.1843**	0.1087	0.0912	0.0699	0.0448	0.0318
	Bus 6	-0.0008	0.0002	0	0	-0.0001	**0.1087**	0.0912	0.0699	0.0448	0.0318
	Bus 7	-0.0147	0.003	0	-0.0001	-0.0005	0.0005	**0.092**	0.0696	0.0448	0.032
	Bus 8	0.0069	-0.0014	0	0	0.0002	0	0.0002	**0.0703**	0.0447	0.0317
	Bus 9	-0.0025	0.0005	0	0	-0.0001	0	0	0.0001	**0.0448**	0.0318
	Bus10	0.0016	-0.0003	0	0	0	0	0	0	0.0001	**0.0319**

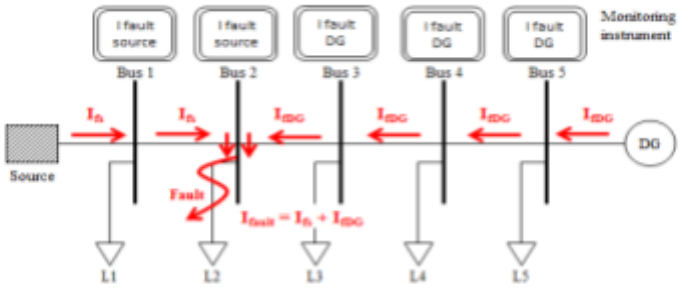

Figure 9. Explanatory image of fault current flows in a single source radial system with DG

Based on result observed in Figure 10, to predict all buses current magnitude during fault, two monitor placement need to be performed. One unit monitor need to be placed at bus 1 (near to the source) in order for RBFNN to accurately predict current at bus 1 to bus 5. While another one unit monitor need to be placed at bus 10 (near to DG) for accurate current magnitude's prediction for bus 7 to bus 10. Therefore, in 10 bus system with DG, bus 1 and bus 10 will be set as monitored bus, while bus 2, 3, 4, 5, 6, 7, 8, and 9 will be set as unmonitored buses.

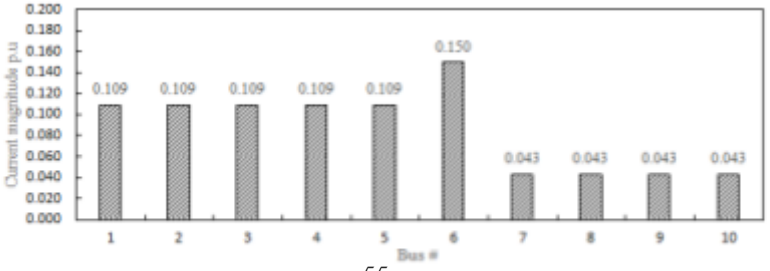

Figure 10 Current magnitude at each bus during LG fault (R_f=0) simulated at bus 6

Figure 11 shows the structure of RBFNN for 10 bus system with DG with 2 unit monitor placement. The numbers of neuron for input and output layers are 2 and 8, respectively. The hidden layer of radial basis contains 50 neurons while linear layer contains 8 neurons.

Figure 11. RBFNN structure for 10 bus system with DG

Table 7 shows the performance analysis of the developed RBFNN for various values of spread constant. The best spread constant for 10 bus system with DG is found to be 0.5. The best performance shows result of 4.87E-04 for SSE, 0.9994 for R^2 and 2.50E-03 for RMSE. Figure 12 shows regression plots of spread constant of 1 and 0.1 for the developed RBFNN. Referring Figure 12, predicted data can be seen most fit the simulated data with spread constant 0.5.

Table 7. RBFNN performance for 10 bus system with DG with different spread constant

Spread constant	SSE	R^2	RMSE
100	4.01E-01	0.4823	6.75E-02
50	3.20E-01	0.7143	6.03E-02
1	2.02E-01	0.8523	4.79E-02
0.5	8.06E-02	0.9464	3.03E-02
0.1	4.74E+00	0.2254	2.32E-01

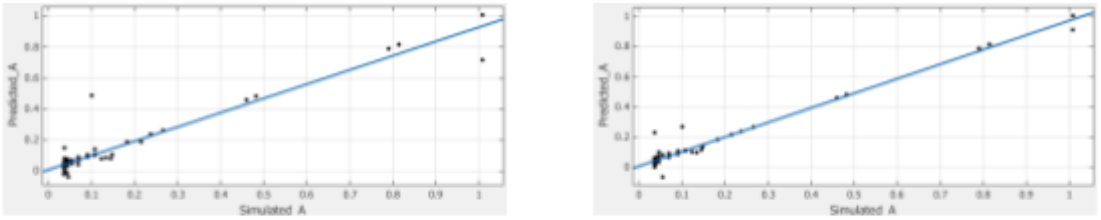

(a) Spread = 1 (b) Spread = 0.5

Figure 12. Regression plots of simulation results versus RBFNN predicted results with different spread constant

With spread constant of 0.5, RBFNN has predicted current magnitude for bus 2 to bus 9 of 10 bus system with DG almost accurately. Comparison of Table 8 and 9 shows that diagonal predicted current magnitude values were very close to the simulation values. Diagonal current values shows maximum values compared to other magnitudes in the same column – which will indicates faulty bus. Based on pattern of predicted current magnitude at buses, it can be seen

possible to identify faulty buses using the predicted data. It was proven that fault detection in term of faulty bus can be identified by current magnitude pattern at buses during fault with only two monitor placements in system with DG.

Table 8. Simulated data of 10 bus system with DG for RBFNN test sample ($R_f = 0.15\Omega$)

		Faulty bus									
		Bus 1	Bus 2	Bus 3	Bus 4	Bus 5	Bus 6	Bus 7	Bus 8	Bus 9	Bus 10
M	Bus 1	**1.008**	0.78992	0.45964	0.23721	0.18263	0.10778	0.09044	0.06932	0.04439	0.03735
o		0.03704	**0.81359**	0.45957	0.23718	0.18261	0.10778	0.09044	0.06932	0.04437	0.03738
n	Bus 2	1	**2**	4	7	8	4	5	7	8	4
i		0.03736	0.03625	**0.48229**	0.23722	0.18263	0.10777	0.09043			0.03727
t	Bus 3	6	2	**9**	2	4	1	2	0.06931	0.04441	6
o		0.03769	0.03630	0.03428	**0.26549**		0.10773	0.09042	0.06930	0.04412	0.03725
r	Bus 4	3	5	1	**7**	0.18246	3	6	6	3	4
i		0.03558		0.03889	0.03681	**0.21589**	0.10806	0.09049	0.06941	0.04617	0.04063
n	Bus 5	1	0.03613	5	7	**4**	3	8	5	7	9
g		0.03988	0.03655	0.02992	0.03354	0.03539	**0.14737**	0.09014	0.06893	0.04042	0.02802
a	Bus 6	1	6	2	6	4	**7**	7	4	2	3
t		0.03404	0.03587		0.03929	0.03986	0.04408		0.07004	0.05100	0.05337
b	Bus 7	1	5	0.04219	6	7	9	**0.13499**	3	1	7
u		0.03794			0.03486	0.03636	0.04231	0.04595	**0.12308**	0.04265	0.03296
s	Bus 8	9	0.03641	0.03375	4	8	9	5	**9**	6	5
			0.03628	0.03511	0.03571	0.03707	0.04265	0.04610	0.05490	**0.14495**	0.03771
	Bus 9	0.03736	9	6	9	6	3	2	5	**4**	1
	Bus1										
0		0.03735	0.03628	0.03511	0.03572	0.03706	0.04268	0.04609	0.05493	0.10062	**1.008**

Table 9. RBFNN predicted data of 10 bus system with DG for RBFNN test sample ($R_f = 0.15\Omega$)

		Faulty bus									
		Bus 1	Bus 2	Bus 3	Bus 4	Bus 5	Bus 6	Bus 7	Bus 8	Bus 9	Bus 10
M	Bus 1	**1.008**	0.78992	0.45964	0.23721	0.18263	0.10778	0.09044	0.06932	0.04439	0.03735
o		0.03704	**0.81359**	0.45957	0.23718	0.18261	0.10778	0.09044	0.06932	0.04437	0.03738
n	Bus 2	1	**2**	4	7	8	4	5	7	8	4
i		0.03736	0.03625	**0.48229**	0.23722	0.18263	0.10777	0.09043			0.03727
t	Bus 3	6	2	**9**	2	4	1	2	0.06931	0.04441	6
o		0.03769	0.03630	0.03428	**0.26549**		0.10773	0.09042	0.06930	0.04412	0.03725
r	Bus 4	3	5	1	**7**	0.18246	3	6	6	3	4
i		0.03558		0.03889	0.03681	**0.21589**	0.10806	0.09049	0.06941	0.04617	0.04063
n	Bus 5	1	0.03613	5	7	**4**	3	8	5	7	9
g		0.03988	0.03655	0.02992	0.03354	0.03539	**0.14737**	0.09014	0.06893	0.04042	0.02802
a	Bus 6	1	6	2	6	4	**7**	7	4	2	3
t		0.03404	0.03587		0.03929	0.03986	0.04408		0.07004	0.05100	0.05337
b	Bus 7	1	5	0.04219	6	7	9	**0.13499**	3	1	7
u		0.03794			0.03486	0.03636	0.04231	0.04595	**0.12308**	0.04265	0.03296
s	Bus 8	9	0.03641	0.03375	4	8	9	5	**9**	6	5
			0.03628	0.03511	0.03571	0.03707	0.04265	0.04610	0.05490	**0.14495**	0.03771
	Bus 9	0.03736	9	6	9	6	3	2	5	**4**	1
	Bus1										
0		0.03735	0.03628	0.03511	0.03572	0.03706	0.04268	0.04609	0.05493	0.10062	**1.008**

Similar approach has been applied and tested on 34 bus radial distribution systems. In 34 bus systems, due to the existence of several branches in system, network zoning becomes important to let RBFNN accurately predict current magnitude at unmonitored buses.

3.3 34 Bus Radial Distribution System Without DG

Two types of 34 bus radial distribution system have been tested, namely 34 bus system without DG and 34 bus system with DGs. These test models are single source models and consists of four branches. Approach in fault location

detection in term of faulty bus for both systems has been discussed and method of fault detection using RBFNN for each system has been proposed.

Six data sets with various R_f has been generated using Power World fault analysis for 34 bus system without DG. Five data sets have been used for RBFNN training, while one data set has been used for RBFNN testing.

Network zoning has been performed based on consideration of; one zone shall consist of one current source during fault. For example, consider that LG fault has occurred at bus 15. In this case, current will flow from source, flowing through bus 13, bus 14, bus 15 and finally to the ground. Bus 13 is the first bus in the branch, so bus 13 is considered as current source bus during fault occurrence. Therefore, Zone 2 will cover from bus 13 which is current source bus until bus 16 which is the last bus in the particular branch. Figure 13 shows zoning for 34 bus network without DG. The 34 bus system without DG has been divided into five network zones. Table 10 shows network zoning and related bus number for this network.

Table 10. Network zoning for 34 bus radial system without DG

Zone	Bus number
1	Bus 1 – Bus 12
2	Bus 13 – Bus 16
3	Bus 17 – Bus 27
4	Bus 28 – Bus 30
5	Bus 31 – Bus 34

All possible current flows during fault need to be identified in order to select the most suitable monitored buses. Monitored buses shall be buses which will act as current source during fault. There are five current source buses in this network, namely bus 1, bus 13, bus 17, bus 28 and bus 31. Table 11 shows monitored and unmonitored buses for each zone.

Table 11. Monitored and unmonitored bus for each zone of 34 bus system without DG

Zone	Monitored bus number	Unmonitored bus number
1	Bus 1	Bus 2, 3, 4, 5, 6, 7, 8, 9, 10, 11, 12
2	Bus 13	Bus 14, 15, 16
3	Bus 17	Bus 18, 19, 20, 21, 22, 23, 24, 25, 26, 27
4	Bus 28	Bus 29, 30
5	Bus 31	Bus 32, 33, 34

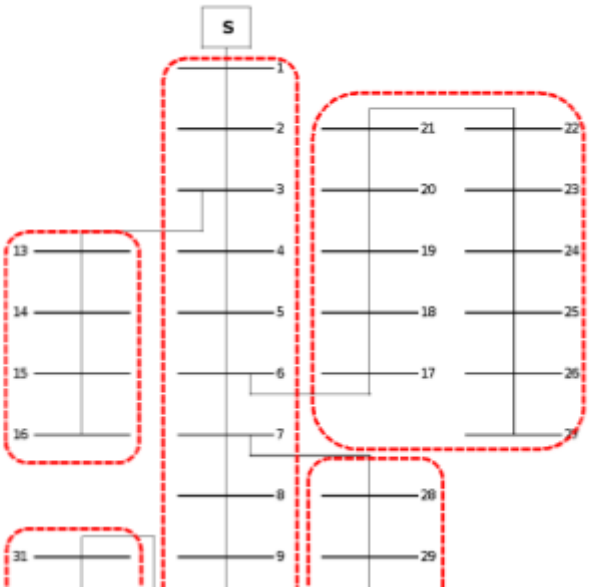

Figure 14 shows the structure of RBFNN for 34 bus system without DG with 5 unit monitor placement. The numbers of neuron for input and output layers are 5 and 29, respectively. The hidden layer of radial basis contains 170 neurons while linear layer contains 29 neurons.

Figure 14. Structure of RBFNN for 34 bus system without DG

Table 12 shows the performance analysis of the developed RBFNN for various values of spread constant. Generally, SSE and RMSE results were generally not good by all spread constant – shows that the predicted data were not fit with the simulated data.

Table 12. RBFNN performance for 34 bus system without DG with different spread constant

Spread constant	SSE	R^2	RMSE
5	2.336	0.9224	4.87E-02
1	1.36	0.9558	3.72E-02
0.5	1.212	0.9613	3.51E-02
0.1	1.645E+03	0.0204	1.293
0.05	7.981E+05	0.0005	28.48

Figure 15 shows regression plots of spread constant of 0.05, 0.1, 0.5 and 1 for the developed RBFNN. Referring to Figure 15, it can be observed that, RBFNN can't correctly predict the simulated value of 0 p.u. magnitude for this network. Data were extremely scattered for 0 p.u magnitudes, while RBFNN can be seen have no problem to predict other magnitude values. To improve accuracy of results several trials and approaches have been taken such as; increase training data sets, increase number of monitored buses, rearrangement of training input and target data. However, it was found that the prediction of 0 p.u. magnitudes were still inaccurate. Further study need to be done to improve RBFNN in order to increase accuracy of prediction for this network.

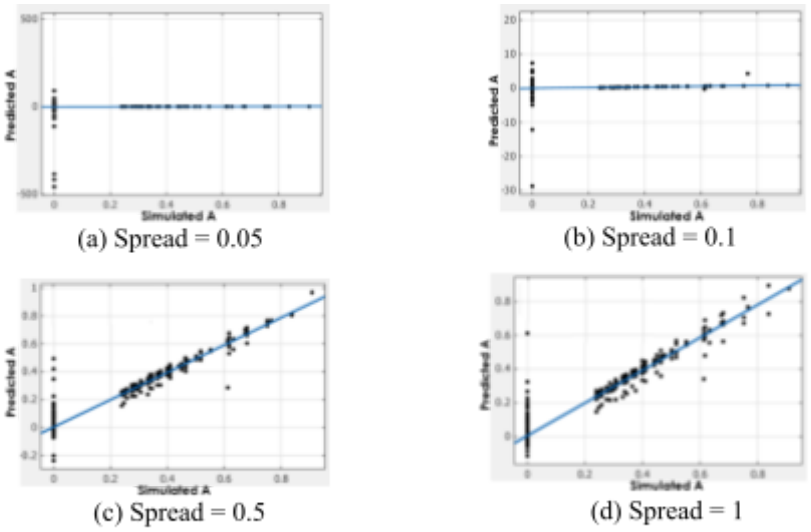

(a) Spread = 0.05 (b) Spread = 0.1

(c) Spread = 0.5 (d) Spread = 1

Figure 15. Regression plots of different spread constant for RBFNN predicted versus simulated result of 34 bus system without DG

3.4 34 Bus Radial Distribution System With DG

Seven data sets with various R_f has been generated using Power World fault analysis. Six data sets have been used for RBFNN training, while one data set has been used for RBFNN testing.

Based on approach on network without DG for network zoning, similar approach has been taken to perform network zoning for network with DG. Figure 16 shows zoning for 34 bus network with DG. The 34 bus system without DG has been divided into six network zones. Table 13 shows network zoning and related bus number for this network.

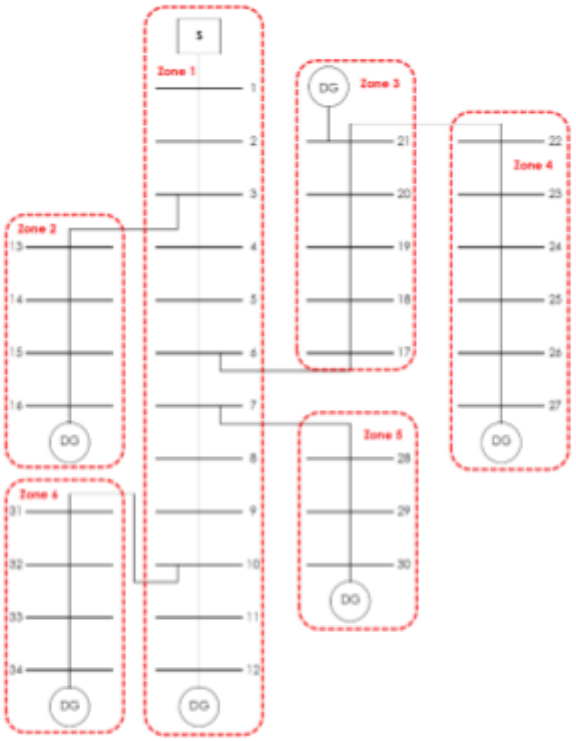

Figure 16. The 34 bus system with DG after performing network zoning

Table 13. Network zoning for 34 bus system with DG

Zone	Bus number
1	Bus 1 – Bus 12
2	Bus 13 – Bus 16
3	Bus 17 – Bus 21
4	Bus 22 – Bus 27
5	Bus 28 – Bus 30
6	Bus 31 – Bus 34

As what has been learned in previous section, monitored buses shall be buses which will act as current source during fault. There are twelve current source buses in this network, namely bus 1, 12, 13, 16, 17, 21, 22, 27, 28, 30, 31 and 34. Table 14 shows monitored and unmonitored buses for each zone. To achieve accurate result, 13 monitored buses and 21 unmonitored buses for 34 bus network with DGs has been selected.

Table 14. Monitored and unmonitored bus for each zone of 34 bus system with DG

Zone	Monitored bus number	Unmonitored bus number
1	Bus 1, 12	Bus 2, 3, 4, 5, 6, 7, 8, 9, 10, 11
2	Bus 13, 16	Bus 14, 15
3	Bus 17, 20, 21	Bus 18, 19
4	Bus 22, 27	Bus 23, 24, 25, 26
5	Bus 28, 30	Bus 29
6	Bus 31, 34	Bus 32, 33

Figure 17 shows the structure of RBFNN for 34 bus system with DG with 13 unit monitor placement. The numbers of neuron for input and output layers are 13 and 21, respectively. The hidden layer of radial basis contains 204 neurons while linear layer contains 21 neurons.

Figure 17. Structure of RBFNN for 34 bus system with DG

Table 15 shows the performance analysis of the developed RBFNN for various values of spread constant. The best spread constant for RBFNN in 34 bus system with DG is found to be 11. The best performance shows result of 4.38E-02 for SSE, 0.9958 for R^2 and 7.84E-03 for RMSE.

Figure 18 shows regression plots of spread constant of 1, 5, 10 and 11 for the developed RBFNN. It can be observed that, by changing spread constant for RBFNN, predicted data will scatter accordingly and accuracy of predicted data changes.

Table 15. RBFNN performance for 34 bus system with DG with different spread constant

Spread constant	SSE	R^2	RMSE
15	8.28E-02	0.9920	1.08E-02
13	8.06E-02	0.9922	1.06E-02
12	4.54E-02	0.9957	7.98E-03
11	4.38E-02	0.9958	7.84E-03
10	4.42E-02	0.9958	7.88E-03
8	4.56E-02	0.9956	8.00E-03
5	5.71E-02	0.9946	8.95E-03
1	2.95E-01	0.9724	2.03E-02

The RBFNN predicted data then has been arranged into table to find faulty buses via pattern. The highest current magnitude in column will indicate that the particular bus is a faulty bus. The predicted result for 34 bus network with DG is given in Appendix C Table C1.

Referring to Table C1, all faulty buses were showing the highest magnitude of current compared to other buses in the same column. It was shown that the faulty buses can be identified by the proposed approach by 100%.

It was found that it is possible to detect fault location in term of faulty bus by only several monitor placements in distribution system for LG fault. In a network system with DG, additional monitor placements were required to achieve greater accuracy in RBFNN prediction.

In a radial system with DG, current can be seen flowing from various directions. Therefore, current magnitude at faulty bus (fault current) was higher compared to system or network without DG.

It was also found that, network zoning and monitor placement can affect RBFNN prediction accuracy. In 10 bus system without DG, only 1 monitor placement was needed, while in 10 bus system with DG, 2 monitor placements were required to predict current magnitudes at buses during LG fault. In a larger system, only 13 monitor placements were required in 34 bus network with DGs. Finally, with accurate current magnitude prediction by RBFNN, faulty bus can be identified via current magnitude pattern at buses during fault.

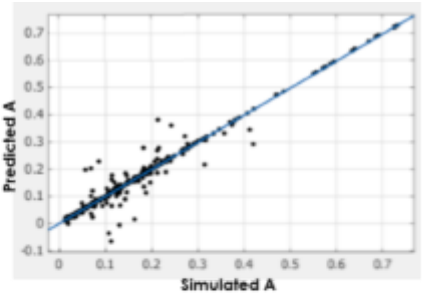

(a) Spread = 1

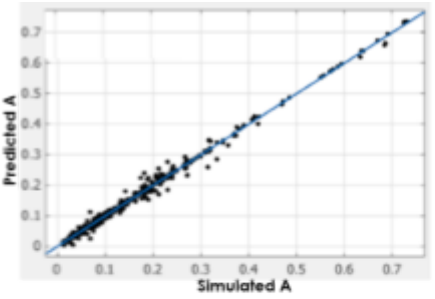

(b) Spread = 5

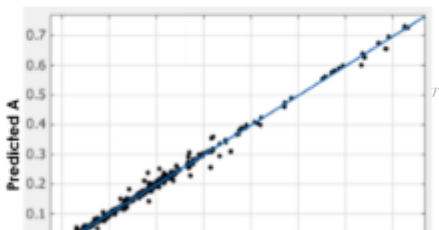

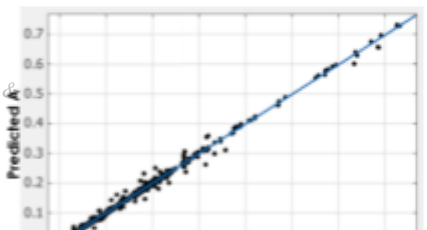

raphy System &

4. Conclusion

It was found that it is possible to detect fault location in term of faulty bus by only several monitor placements in distribution system for LG fault using RBFNN. With accurate current magnitude prediction at buses using RBFNN, faulty bus can then be identified via current magnitude pattern during fault of each particular network.

In a larger network system, correct network zoning and monitor placement selection is required to get greater RBFNN prediction accuracy. To select the best monitor to be placed in system, all possible current flow during fault first need to be identified. Monitored buses shall be buses which will act as current source during fault. With proper network zoning and monitor placement, current magnitude prediction for all buses in radial distribution system can be performed accurately by RBFNN. Also, with the consideration on monitor placement in this study, minimum monitor placement has been achieved for all test models; namely, 10 bus single radial distribution system without DG, 10 bus single radial distribution system with DG and 34 bus radial distribution system with DG. With accurate prediction of current magnitude by RBFNN, faulty bus can be identified by arranging all predicted data into table and observe current magnitude patterns during fault. The bus with highest magnitude of current is the faulty bus.

However, lower accuracy result was shown in 34 bus network without DG even though same approach has been applied to predict current magnitudes at buses. RBFNN inaccuracy for this network can be seen caused by inability of RBFNN to accurately predict 0 p.u. current magnitudes at buses. This is perhaps due to limitation of nntool in MATLAB, and further study to improve accuracy of RBFNN prediction need to be conducted.

5. References

[1] Ray, Subir. 2007. *Electrical Power Systems: Concepts, Theory and Practice.* Prentice Hall of India Private Ltd.,
[2] S.M, Azharuddin. 2014. A near accurate Solar PV Emulator Using dSPACE controller for real time control. 61, *Energy Procedia*.: 2640-2648.
[3] Juan M. Gers, Edward J. Holmes. 2005. Protection of Electricity Distribution Networks. 2nd. The Institution of Engineering and Technology, IET, 2005. *Power and Energy Series 47*.
[4] Mert Korkah, Hanoch Lev-Ari, Ali Abur. 2012. Travelling-Waved-Based Fault-Location Technique for Transmission Grids via Wide-Area Synchronized Voltage Measurements. *IEEE Transactions on Power Systems.* Vol.27, No.2
[5] F.M. Abo-Shady, M.A. Alaam, Ahmed M. Azmy. 2013. Impedance-Based Fault Location Technique for Distribution Systems in Presence of Distributed Generation. *IEEE International Conference on Smart Energy Grid Engineering (SEGE*), Oshawa, 2013.
[6] K. W. Min, S. Das, S. Santoso. 2016. Improved Method for Locating Faults Upstream from Distributed Generation. Department of Electrical and Computer Engineering, The University of Texas at Austin. IEEE 2016.
[7] Power System Relaying Committee. 2014. IEEE Guide for Determining Fault Location on AC Transmission and Distribution Lines. 2014*, IEEE Std* C37.114.

[8] L.L. Lai, T.F. Chan. 2007. *Distributed Generation: Induction and Permanent Magnet Generators*.John Wiley & Sons Ltd.,
[9] Suchimita S. Duttagupta, Chanan Singh. 2006. A reliability assessment methodology for distribution system with distributed generation. *IEEE General Meeting*, Montreal, Canada, 2006.
[10] Sustainable Energy Development Authority Malaysia. [Online] [Cited: November 28, 2016.] http://www.seda.gov.my/.
[11] Hadi Zayandehroodi, Azah Mohamed, Hussein Shareef, Marjan Mohammadjafari. 2011. An automated protection method for distribution network with distributed generations using radial basis function neural network. *Power Engineering and Optimization Conference (PEOCO*), 2011. 255-260.
[12] Hussein Shareef, Azah Mohamed. 2013. An alternative voltage sag source identification method utilizing Radial Basis Function Network. *22nd International Conference on Electricity Distribution*, Stockholm 2013.
[13] Siti Hajar Ibrahim, Hussain Shareef, Azah Mohamed, Ahmad Asrul Ibrahim. 2014. Monitor Placement for Fault Location in Radial Distributed Network based on Current Sensitivity and System Topology. *Australian Journal of Basic and Applied Sciences,* Vol. 8(19): 60-63.
[14] M.M. Saha, J. Izykowski, E. Rosolowski. 2010. *Fault Location on Power Networks*. London : Springer.
[15] M.S. Naidu, V. Kamaraju. 2004. *High Voltage Engineering*, McGraw-Hill
[16] Y. Li, Q. Du, X. Qi, Q. Pang, G. Zhu. 2011. A review of Single-Line-to-Ground Fault Lcation Methods in Distribution Networks. *4th International Conference on Electric Utility Deregulation and Restructuring and Power Technologies* 2011.
[17] Jose Cordova, M. Omar Faruque. 2015. Fault Location Identification in Smart Distribution Networks with Distributed Generation. *North American Power Symposium (NAPS)* 2015: 1-7.
[18] Nor Azliana Abdullah, Saifulnizam Abd Khalid. 2016. *Voltage sag source location using Artificial Neural Network*. Faculty of Electrical Engineering, Universiti Teknologi Malaysia.
[19] R. S. Rao, S.V.L. Narasimham, M. Ramalingaraju. 2011. Optimal Capacitor Placement in a Radial Distribution System using Plant Growth Simulation Algorithm. *Electrical Power and Energy Systems*. 33: 1133-1139.
[20] M. Chis, M.M.A. Salama, S. Jayaram. 1997. Capacitor placement in distribution system using heuristic search strategies. *IEE Proceedings – Generation Transmission Distribution* 144 (3): 225 – 230.
[21] K.R. Wagiman, S.N. Khalid, H. SHareef. 2017. Location of voltage sag source by using Artificial Neural Network. *Jurnal Teknologi (Sciences & Engineering)* 79:2 11-30.
[22] Hadi Saadat. 1999. *Power System Analysis*. McGraw-Hill.